NEW METHODOLOGIES FOR INVESTIGATING RILLENKARREN CROSS-SECTIONS: A CASE STUDY AT LLUC, MALLORCA

J. CROWTHER

Department of Geography, University of Wales, Lampeter, Ceredigion, SA48 7ED, UK

Received 24 September 1996; Revised 26 April 1997; Accepted 14 May 1997

ABSTRACT

Precise data on the detailed form of 108 rillenkarren (flute) cross-sections at Lluc have been obtained by digitizing photographic enlargements of profile gauge traces taken in the field. Such data enable morphometric analysis to be undertaken more rigorously and on a wider range of characteristics (e.g. flute and cusp asymmetry, surface roughness and the properties of vertical sections) than in previous studies. Methods for quantifying and investigating these characteristics are presented. Since many of the flutes were found to be asymmetrical, the two 'sides' of each flute have been analysed separately. Although most of the sides have characteristic parabolic profiles, about one-fifth are rectilinear in form. The parabolic sides are relatively smooth, and this is thought to be attributable to dissolution within the thin film of water present on the surface during rainfall and/or to the detachment of small protruding fragments of limestone (weathered loose by biological agencies) by raindrop impact. The rectilinear sides have distinctly rougher surfaces and are thought to be truncated or immature forms. Sets of rillenkarren on rock outcrops appear to be in dynamic equilibrium, maintaining their overall form over time, but changing in detail as cusp lines shift, existing flutes are captured and new ones are initiated.

Earth surf. process. landforms, **23,** 333–344 (1998)
No. of figures: 4 No. of tables: 5 No. of refs: 17
KEY WORDS: karst; rillenkarren; morphometry; cross-sections; surface roughness

INTRODUCTION

Rillenkarren are highly distinctive dissolutional forms that develop on limestone, gypsum and salt. They occur as tightly packed sets of parallel flutes (Figure 1a) that extend from the crest of rock outcrops for up to a metre or so downslope, before petering out into a planar surface (termed 'ausgleichsfläche'). Characteristically, the individual flutes are parabolic in cross-section and are separated by sharply pronounced cusp lines. Laboratory simulation studies on plaster of Paris blocks have shown that rillenkarren are products of direct rainfall, the concave parabolic form being very effective in intercepting rainfall by deflecting the parallel forces of raindrop impact into water flowing down the centre of the flute (Glew and Ford, 1980). The flutes are thought to extend downslope until the thickness of the water film becomes sufficient to absorb raindrops without them impacting directly on the underlying rock surface. Clearly, the distance downslope at which the critical thickness is reached increases on steeper slopes as a result of lower rainfall input per unit area and increased velocity of flow. Studies of both simulated forms (Glew and Ford, 1980) and natural rillenkarren at Lluc, Mallorca (Mottershead, 1996), confirm the direct relationship between slope angle and rillenkarren length. Until recently, dissolution was assumed to be the only process by which rillenkarren erode. However, experimental simulation and scanning electron microscopy studies (Fiol *et al*., 1996) have shown that algae can play a significant role in the weathering process on limestone by weakening the structure of the surface, thereby allowing raindrop impact to dislodge fine rock particles.

According to Ford and Lundberg (1987, p. 122) rillenkarren display 'remarkable regularity of form and dimension'. This uniformity is certainly striking when rillenkarren in different geographical regions are compared. For example, compilations of world data reveal mean widths on limestone to be mostly between 15 and 20 mm (Ford and Lundberg, 1987; Goudie *et al*., 1989). However, observation of sets of rillenkarren on individual rock surfaces suggests that width and depth can vary markedly from one flute to the next. Moreover,

CCC 0197-9337/98/040333–12 $17.50

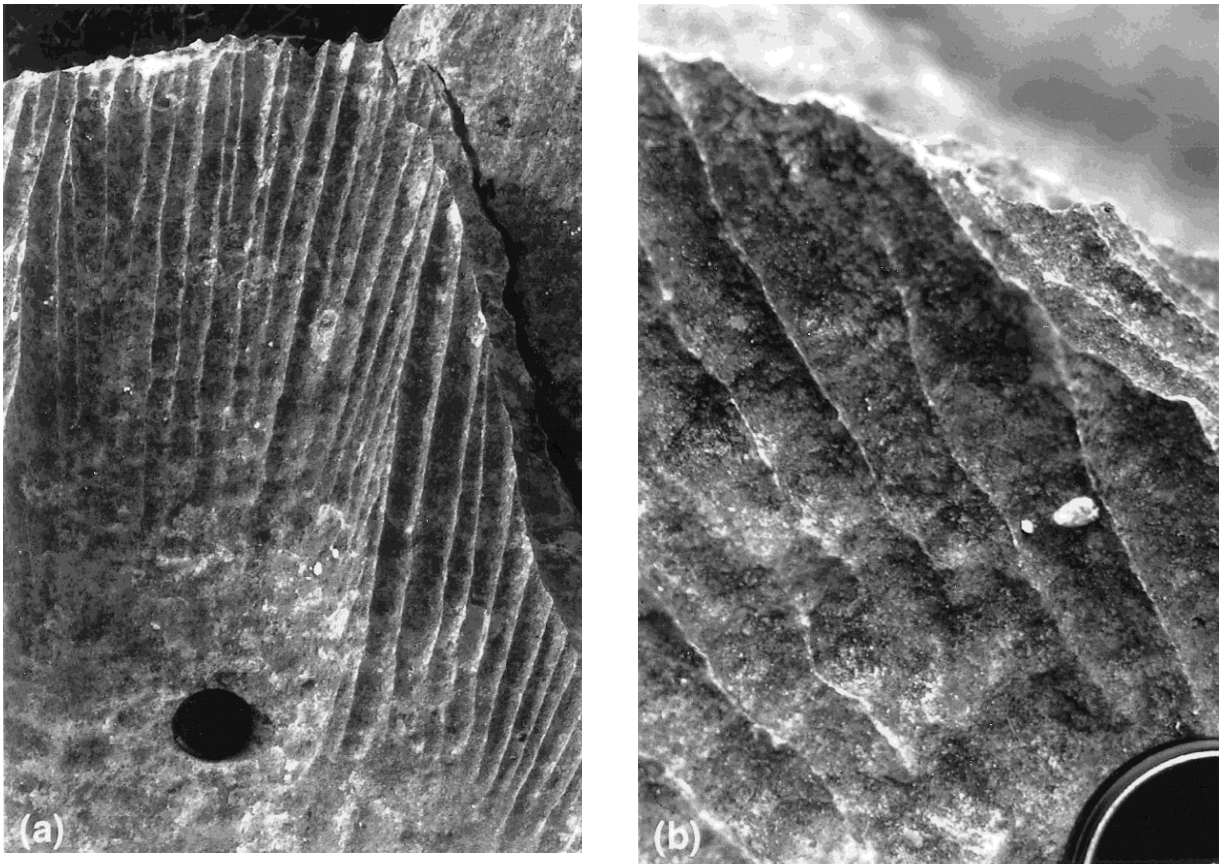

Figure 1. (a) Typical ridge crest with rillenkarren (flutes) fading out into an ausgleichsfläche (planar surface); the lens cap is 54 mm in diameter. (b) Close-up of flutes showing the detailed form of the surface and presence of occasional arenaceous gravels. NB. None of the profile gauge transects studied included arenaceous pebbles/gravels or >2 mm quartz grains

the flutes themselves, rather than being symmetrical and smooth in cross-section, are often quite asymmetrical and have rough, irregular surfaces (Figure 1b). Such local variability is evident in published profiles of natural rillenkarren (e.g. Lundberg, 1977a; Dunkerley, 1979; Goudie *et al.*, 1989; Mottershead, 1996) and simulated forms (Glew and Ford, 1980). Hitherto, no attempt has been made to quantify such variability or to assess its significance. Recent work, for example, has highlighted surface roughness as an important distinguishing characteristic of different karren types (Crowther, 1997), but this property has not been investigated in relation to rillenkarren cross-sections.

The present study develops appropriate methodologies for examining local variability in rillenkarren morphometry, and illustrates their use with reference to 108 rillenkarren cross-sections on limestone at Lluc. In particular, it seeks: (i) to establish the extent to which individual flutes and the cusp lines that separate them are asymmetrical in form; (ii) to determine the precise form and 'goodness of fit' of curves for each side of individual flutes – curve fitting in previous studies has been done by eye, e.g. using transparent overlays of sets of curves (Dunkerley, 1979), and has been undertaken on entire cross-sections, which is inappropriate for asymmetrical profiles; (iii) to examine the form of vertical sections, in addition to the conventional cross-sections, since this is the 'true' form with which (vertically falling) raindrops actually interact; and (iv) to investigate the amount of surface roughness that is superimposed upon the underlying cross-sectional 'shape'.

FIELD AREA

The study area is located on a sparsely vegetated south-facing slope in the Serra de Tramuntana, 0·5 km east of the Monasterio de Lluc and at an altitude of 500 m above sea level. The limestone, of Oligocene/Lower

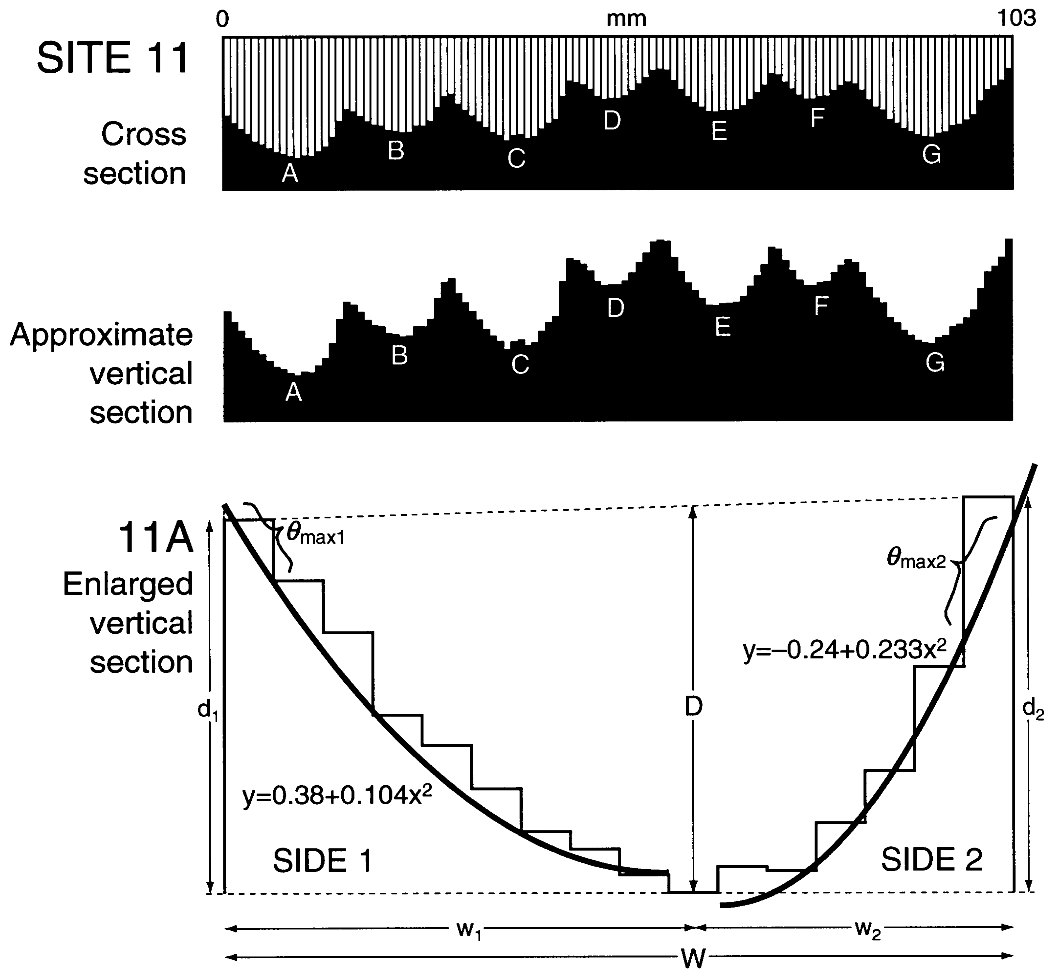

Figure 2. Illustration of the form of the rillenkarren sections and approximate vertical sections recorded. The enlarged vertical section of 11A (excluding the rods that coincide with the cusps) shows the best-fit parabolic curves fitted to the upslope corners of each rod. Key morphometric properties: D and W = depth and width of flute; d_1, d_2, w_1, w_2 = depths and widths of the sides; θ_{max1} and θ_{max2} = the gradient of the best-fit curve between the penultimate and end point of the profile gauge transect

Miocene age, comprises hard clastic limestone breccias and conglomerates. These have a variable fine-grained fabric, a consistently low Mg concentration (Mg:Ca+Mg, <0·02) and variable concentrations of insoluble impurities (1·14–10·1 per cent), based on data presented in Mottershead (1996) and Crowther (1997). These characteristics predispose the rock to the development of surface irregularities as weathering proceeds. Locally, quartz granules (up to pea size) and arenaceous pebbles stand proud of the surface (Figure 1b; Mottershead, 1996). The meso-topography is dominated by steep-sided ridges and pinnacle-like outcrops, the crests of which display well developed rillenkarren (Figure 1a). The area experiences a typical Mediterranean climate: mean annual temperature 13·6°C and annual precipitation 1185 mm (Mottershead, 1996).

METHODOLOGICAL CONSIDERATIONS

Sampling strategy and recording of cross-sections

Twenty surfaces containing fully developed rillenkarren (i.e. with an ausgleichsfläche downslope) were selected at random. The only sites excluded were those where profile gauge transects (see below) would have included exposed arenaceous pebbles/gravels or >2 mm quartz grains. At each point measurements were

confined to a section of rock encompassing a *set* of typically four to seven flutes (Figure 2). The slope (θ_c) and length of the central flute were measured, along with the slope of the ausgleichsfläche (θ_{agf}). θ_c is taken as the overall slope for the rillenkarren set.

The form of the cross-profiles for each set was determined at a position midway down the central flute using a standard 150 mm carpenter's profile gauge, with 165 cylindrical, square-ended rods. Measurements were made orthogonal to the general slope of the surface (here termed *cross-sections*). High levels of precision (+/− 0·025 mm) were achieved by photographing the configuration of the rods in the field and then digitizing the height of the rods (y_i) from photographic enlargements. In each case the upslope corner of the rod was taken to be the point of contact (x_i). This method provides greater accuracy and precision than can be obtained by tracing the shape onto paper in the field (cf. Dunkerley, 1979; Haigh, 1981; Vincent, 1983), which inevitably tends to smoothen out minor irregularities. Moreover, by determining the coordinates of each rod tip, quantitative analysis can be undertaken on a wider range of properties than has been possible in previous studies.

Ideally, the vertical section would have also been recorded, since this is the actual form with which water interacts. Unfortunately, on steeper outcrops the rods tend to slide over the surface and the results are unreliable. Approximate *vertical sections* have therefore been derived from the height values (y_i) of the cross-sections as $y_i/\cos\theta_c$.

Limitations of profile gauge traces

It should be recognized that the resolution of the profile produced is dependent upon the thickness of the rods (mean diameter 0·91 mm). In the case of rillenkarren cross-sections, three specific limitations also need to be considered. First, while the point of contact between the rods and the rock surface will generally be on the upslope side, there will be inconsistencies where the profile is flatter or more irregular in form. Secondly, the accuracy with which the lowest point of a flute is determined is constrained by the thickness of the rods (depth is almost invariably underestimated), and by variations in the transverse location of the rods in relation to the cross-section (i.e. different profiles would be recorded if the gauge were positioned slightly to the left or right). Finally, unless the cusp between adjacent flutes is sharp and happens to coincide with a point exactly between two rods, then the profile generated underestimates the gradient of the top of both adjacent sides, producing a flattening effect on the cusps. To overcome the latter problem, the topmost rod has been eliminated in all determinations except flute width, where the width of the rod on each cusp has been split evenly between the adjacent flutes (Figure 2). The advantages of this procedure greatly outweigh any minor errors in the resulting width and depth data. Interestingly, this problem does not seem to have been addressed in previous studies and could, for example, explain why Dunkerley (1979, p. 337) found that many cusps fell below the best-fit circular arcs fitted to the cross-sections. Clearly, the above limitations affect the accuracy of the individual profiles, but the overall effects are likely to be small when the sample size is large.

Basic morphometric variables

As in previous studies, the overall width (W), depth (D) and depth:width (D/W) ratio of flute cross-sections have been determined. In addition, the flutes are considered to comprise two separate *sides*, each extending from the lowest point of the section to the cusp, and having its own width (w), depth (d) and depth:width (d/w) ratio (Figure 2). The asymmetry of each flute is expressed as the ratio of the larger:smaller dimension of the widths, depths and depth:width ratios of the two sides (termed *width*, *depth* and *depth:width asymmetry indices*, respectively). The latter provides a measure of the relative steepness of the two sides.

Curve fitting

Unlike previous studies, curves have been fitted separately to the two sides of each flute, rather than to the complete cross-section. The bottom of each side (coordinates 0,0) is taken to be the upslope corner of the lowest rod. The curves were determined by least-squares regression using standard linearizing procedures (Shaw and Wheeler, 1985, pp. 200–220), with height (y), horizontal distance of the upslope corner of each rod (x), and various derivatives of y and x as variables. Since successive x and y values are not independent, the statistical significance of the curves cannot be assessed. The coefficient of explanation (r^2) does, however, provide a measure of 'goodness of fit'. Initially, quadratic ($y = a + bx + cx^2$) and power ($y = ax^b$) curves were

investigated. The former proved unsatisfactory in that in many cases b was relatively large, i.e. the base of the curve was displaced laterally from the bottom of the side. The power function is better in some respects since the curves pass through 0,0. However, in doing so, it gives a pre-eminence to the bottom of the side, which is unjustified in view of the height variability that is evident in many of the profiles. The curve $y=a+bx^2$ (an offset power curve that is parabolic in form) overcomes the problems identified with the quadratic and power functions, in that it fixes the base at $x=0$, yet allows variation in the height of the base (a), and this has been used in the present study. It also has the advantage of allowing direct comparison with the parabolic curves fitted by eye in previous studies. In addition, the best-fit line ($y=a+bx$) was determined for each side. The r^2 value, which is inevitably high because of the interdependence of the points along the profiles, is used to establish whether the shape fits more closely a parabolic or rectilinear form. Examples of fitted parabolic curves are presented in Figure 2. It should be noted that the only incongruity that arises from fitting curves/lines separately to the two sides is that there is almost inevitably a small disjunction at the base.

Cusp form: sharpness and asymmetry

The slope of the upper part of the sides of the cross- and vertical sections is an important characteristic of rillenkarren, for three reasons. First, it represents the upward ‘trajectory’ of the rillenkarren sides. Secondly, the surface film of water is thinnest here and, hence, direct interaction between raindrops and the rock surface is greatest. Thirdly, the upper slopes determine the sharpness and asymmetry of the cusp that separates adjacent flutes. Unfortunately, the precise lateral position of the cusps cannot be located using profile gauge traces, and the rods falling on the cusp lines have been eliminated (see above). The data presented are therefore based on approximations of cusp form. Here, the slope (termed θ_{max}) between the end and penultimate measurement point at the top of each side has been derived from the best-fit curve or line (Figure 2). This eliminates the effects of surface roughness (see below), thereby enabling the underlying shape to be isolated. The angle between the two *adjacent slopes* that form the cusp (i.e. $180-\theta_{max1}-\theta_{max2}$) provides a measure of *cusp sharpness*, and the difference in θ_{max} between the two sides is indicative of the degree of asymmetry.

Differences in θ_{max} either side of the cusp are likely to promote different rates of erosion, which will inevitably lead to a lateral shifting of the cusp line through time. Attention here focuses on the vertical sections. If the actual rate of erosional lowering normal to the surface (E) was constant (i.e. independent of slope angle, etc.), then the rate of horizontal backcutting of the surface would be proportional to $\sin\theta_{max}$. Such a situation might obtain, for example, if biological weathering were the only significant process operative. In the case of rillenkarren, the rate of erosion is likely to be dependent to some extent upon the volume of water receipt, which may be taken as proportional to $\cos\theta_{max}$. If E varies with $\cos\theta_{max}$, then the backcutting will be proportional to $\sin\theta_{max}.\cos\theta_{max}$. The value of this function increases from zero on horizontal surfaces, where there is no lateral component of erosion, to a peak of 0·500 at a slope of 45°. Thereafter it decreases to zero at 90°, as diminution in incident rainfall becomes the dominant factor. Detailed process studies are needed to establish the precise mechanisms and controlling factors involved. Here, $\sin\theta_{max}$ and $\sin\theta_{max}.\cos\theta_{max}$ are used as *indices of backcutting* for the two specific circumstances described above, and the asymmetry ratios (higher:lower value of these indices either side of the cusp) are used as crude *indices of lateral cusp movement*.

Roughness indices

Surface roughness may be thought of as being attributable to random irregularities that are superimposed on the underlying ‘shape’ of a feature (Crowther, 1996). At the millimetre scale, as investigated here, this can be readily appreciated through the feel or ‘texture’ of the surface. It should be emphasized that the roughness considered here is confined to that present *within* flutes, i.e. it takes no account of the cusp lines between the flutes. Surface roughness is reflected in the absolute gradient change from one measurement point to the next along a profile. For rectilinear features the mean of the absolute gradient change values (termed *MGC*) provides a good index of roughness (Crowther, 1984, 1996; McCarroll, 1992). With flute cross-sections, however, account has to be taken of the changes in gradient that are related to the underlying shape of the parabolic sides. Accordingly, the MGC for the best-fit curve for each of the parabolic sides has been calculated, based on the same x values (rod spacings) used in recording the profile. This value is then subtracted from the actual MGC to give an *adjusted MGC* which makes due allowance for the shape. Inevitably there are cases (11 of the 172

Table I. Morphometric characteristics of the rillenkarren. The gradient and length data are for the central rillenkarren on each rock surface. Gradient data for the ausgleichsflächen are presented for comparison

	n	Mean	Std dev.	Range	Coeff. var.*
Rillenkarren					
Slope, θ_c (°)	20	51	13·8	28–72	27·1
Length (mm)	20	190	61·3	130–360	32·3
Width† (mm)	20	18·2	5·48	8·3–40·3	30·1
Cross-section					
Depth, D (mm)	108	4·2	2·06	0·9–13·1	49·0
Depth:width, D/W	108	0·24	0·074	0·07–0·41	30·8
Vertical section					
Depth, D (mm)	108	7·3	5·08	1·6–30·0	69·6
Depth:width, D/W	108	0·41	0·190	0·12–1·07	46·3
Asymmetry indices‡					
Width	108	1·52	0·578	1·00–4·33	38·0
Depth	108	1·96	1·19	1·00–7·50	60·7
Depth : width	108	1·63	0·670	1·02–5·01	41·1
Ausgleichsflächen					
Slope, θ_{agf} (°)	20	44	18·7	13–77	42·5

* Coefficient of variation (%) = (std dev./mean) × 100·0
† This is the actual width, which takes into account the width of the rods that fall on the cusp lines. These rods are excluded in determining W and D in the remainder of the table (see text and Figure 2)
‡ Ratio of larger : smaller width, depth and depth : width values for the two sides of the cross-section

parabolic sides) where the measured profile is smoother than that determined from the best-fit curve, and these give a small negative adjusted MGC value (minimum −3·32). For present purposes these are regarded as being perfectly smooth sides and a zero value has been substituted. It should be noted that r^2 values from the regression analysis do not provide a measure of surface roughness, since they take no account of the actual distribution of the residuals along the profile.

RESULTS

Basic characteristics and relationships: rillenkarren and ausgleichsflächen

The central flutes have slopes ranging from 28 to 72° and lengths from 130 to 360 mm (Table I). There are strong correlations between rillenkarren slope ($\cos\theta_c$) and length ($r = -0{\cdot}581$, $p = < 0{\cdot}01$), which supports current theory, and between $\cos\theta_c$ and the slope of the ausgleichsfläche ($r = 0{\cdot}871$, $p < 0{\cdot}001$). In most cases the slope decreases slightly from the rillenkarren to the ausgleichsfläche (maximum difference 19°), though at six sites the slope is either the same or the ausgleichsfläche steeper.

The flute cross-sections have a mean width and depth of 18·2 and 4·2 mm, respectively, and a mean depth:width ratio of 0·24. In vertical section the mean depth increases to 7·3 mm and the depth:width ratio to 0·41. All these properties display considerable variability (Table I), e.g. width ranges from 8·3 to 40·3 mm. In relative terms depth is the most variable, particularly in vertical section (coefficient of variation 69·6 per cent). One-way analysis of variance on the seven rillenkarren sets containing seven or more flutes showed there to be a significant difference in $\log_{10}$ width between the sets ($p < 0{\cdot}05$), but no significant difference in either $\log_{10}$ depth or depth:width. Considering all 20 sets there is no significant correlation between $\cos\theta_c$ and either of the three properties. There is, however, a significant correlation between $\log_{10}$ width and $\log_{10}$ depth ($r = 0{\cdot}766$, $p < 0{\cdot}001$).

Asymmetry of rillenkarren cross-sections

Many of the flutes are asymmetric in cross-section (e.g. Figure 3). Overall, more than two-fifths of the width and about half of the depth and depth:width asymmetry indices are ≥1·5 (Figure 4), the extreme values being 4·33, 7·50 and 5·01, respectively (Table I). As is expected from geometric considerations, no side (left or right) is consistently deeper than the other across individual rillenkarren sets. Moreover, only one set is consistent in

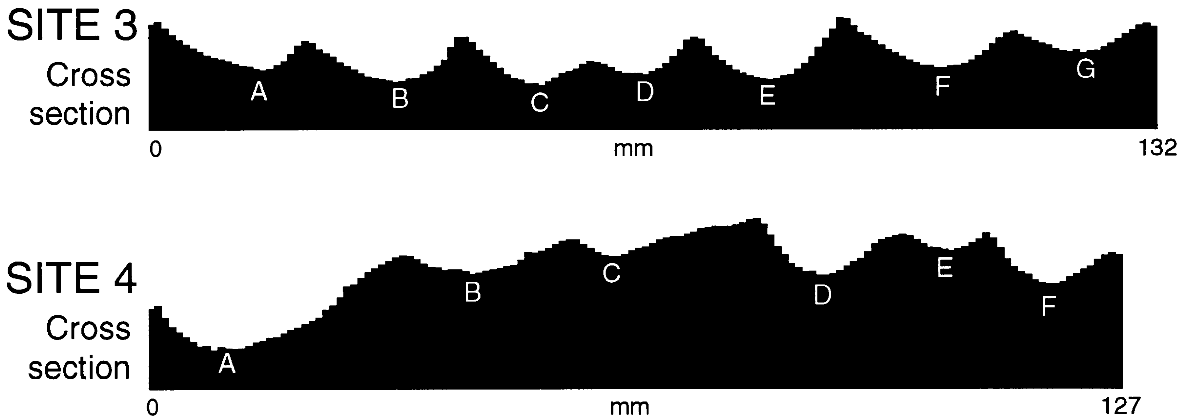

Figure 3. Illustrations of the range of rillenkarren cross-sections encountered in the study. Note the very marked depth, width and depth : width asymmetry of many of the flutes, and the atypical form of sides 4B2 and 4C2. All the sides are parabolic except 3C2, 4B2, 4C2 and 4F2

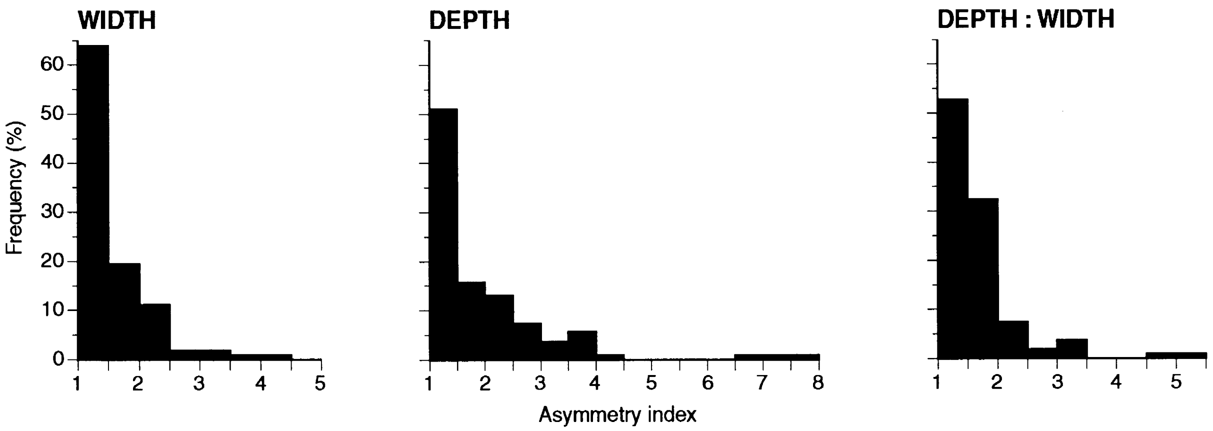

Figure 4. Frequency distribution of asymmetry indices (larger : smaller dimension) for the width, depth and depth : width ratio of the two sides of each flute cross-section ($n = 108$). The asymmetry of the depth : width ratio provides a measure of the relative steepness of the two sides

width asymmetry. Analysis of variance showed there to be no significant difference in the three ($\log_{10}$) asymmetry indices between the sets containing seven or more flutes.

Shapes of rillenkarren sides (cross- and vertical sections)

The widths of the sides and their depths in cross- and vertical section are even more variable than for the rillenkarren as a whole, with coefficients of variation of 40·7, 57·0 and 77·1 per cent, respectively (Table II). The mean slope from cusp to base ranges from 3·0 to 46·0° (mean 25·8°) in cross-section and from 5·0 to 71·7° (38·0°) in vertical section.

The results of the curve-fitting show that 172 (i.e. 79·6 per cent) of the sides are parabolic (Table III). In these cases, r^2 ranges from 0·792 to 0·999, and the b coefficients, which indicate the steepness of the curve, range from 0·0176 to 0·198 in cross-section and 0·0240 to 0·506 in vertical section. The mean b coefficient for the cross-sections (0·0730) is very close to the figure of 0·0745 reported by Mottershead (1996) for mid-flute sections at Lluc. There is a significant inverse correlation between $\log_{10}b$ and $\log_{10}$width ($r = -0{\cdot}658, p < 0{\cdot}001$), which reflects the fact that the wider sides tend to have a more extensive low-gradient basal segment. The remaining 44 sides are rectilinear, with an r^2 of 0·750 to 0·999. Examples of both forms are illustrated in Figure 3. These results support the idea that the parabolic form is dominant. However, with more than 20 per cent of the sides being rectilinear, and 17 of the 20 sets containing at least one such side, the flutes are clearly very variable in cross-section. Compared with the parabolic sides, the rectilinear sides are generally less deeply

Table II. Morphometric characteristics of rillenkaren sides ($n = 216$)

	Mean	Std dev.	Range	Coeff. var.
Width, w (mm)	8·7	3·54	3·2–24·3	40·7
Cross-section				
Depth, d (mm)	4·4	2·51	0·3–17·3	57·0
Mean slope, θ_{mean}* (°)	25·8	8·30	3·0–46·0	32·2
Maximum slope, θ_{max}† (°)				
Parabolic sides‡ ($n = 172$)	43·2	10·3	13·4–60·1	23·8
Rectilinear sides ($n = 44$)	24·3	9·34	3·2–46·3	38·4
Vertical section				
Depth, d (mm)	7·7	5·94	0·4–40·2	77·1
Mean slope, θ_{mean}* (°)	38·0	12·2	5·0–71·1	32·1
Maximum slope, θ_{max}† (°)				
Parabolic sides ($n = 172$)	55·8	11·2	18·3–78·7	20·1
Rectilinear sides ($n = 44$)	37·6	13·9	5·4–71·9	37·0
MGC for rillenkarren cross-sections (°)				
Parabolic sides‡ ($n = 172$)	6·1	4·79	0·0–29·5	78·5
Rectilinear sides ($n = 44$)	9·8	4·17	1·5–20·8	42·6

* Gradient between the top and bottom of the flute side (see Figure 2)
† Gradient between end and penultimate point along profile, as derived from the best-fit parabola or straight line (see Figure 2)
‡ In the case of parabolic sides these are adjusted for curvature (see text)

Table III. Best-fit parabolic curves/lines for sides of the flutes as derived from least-squares regression analysis*

	Mean	Std dev.	Range
Parabolic form ($n = 172$)			
b coefficient† for cross-sections	0·0730	0·0355	0·0176–0·198
b coefficient for vertical sections	0·122	0·0714	0·0240–0·506
Rectilinear form ($n = 44$)			
b coefficient for cross-sections	0·468	0·211	0·057–1·05
b coefficient for vertical sections	0·870	0·530	0·090–3·06

* The coefficient of explanation (r^2) ranges from 0·792 to 0·999 for the parabolic forms and from 0·750 to 0·999 for rectilinear
† b coefficients in the equations $y = a + bx^2$ (parabolic) and $y = a + bx$ (rectilinear), based on values of x and y in mm

incised (t-test: $\log_{10}$ depth, $p < 0·05$; $\log_{10}$ depth:width, $p < 0·05$), but there is no significant difference in width, nor in the gradient (θ_c) of the surface on which they occur. As would be anticipated, the maximum slope (θ_{max}) is significantly greater for parabolic than rectilinear sides (t-test, $p < 0·001$). What is striking, however, is the steepness of θ_{max} for the parabolic sides in vertical section, with *c*. 10 per cent being ≥70° (Table II).

Cusp sharpness and asymmetry

Summary data for the 88 cusps included in the study are presented in Table IV. Cusp sharpness averages 76·4° in vertical section. Inevitably, those cusps with two parabolic sides ($n = 54$) are sharper than those that include rectilinear sides ($n = 34$), the mean values in vertical section being 70·6° and 85·6°, respectively (t-test, $p < 0·01$). The indices of backcutting for the cusp sides range from 0·094 to 0·979 for $\sin\theta_{max}$ and from 0·093 to 0·500 (upper limit of index) for $\sin\theta_{max}.\cos\theta_{max}$. There is marked asymmetry in the sides of many cusps. Thus, the mean difference in slope in vertical section is 13·6° (range, 0·1 to 47·1°), with 22 per cent of the differences being ≥20·0°. This asymmetry is reflected in the high proportions of cusps with indices of lateral cusp movement of ≥1·20: 43 per cent for $\sin\theta_{max}$ and 38 per cent for $\sin\theta_{max}.\cos\theta_{max}$. These findings suggest that many of the cusp lines are likely to shift considerably over time as the flutes are lowered by erosion processes.

Table IV. Morphometric characteristics of the approximate form of rillenkarren cusps in cross- and vertical section

	*n**	Mean	Std dev.	Range
Cusp form				
Cusp sharpness†				
Cross-section (°)	88	101·6	19·1	68·3–154·0
Vertical section (°)	88	76·4	21·5	28·5–139·8
Difference in slope (θ_{max}) between the two sides				
Cross-section (°)	88	13·4	9·02	0·1–44·8
Vertical section (°)	88	13·6	9·79	0·1–47·1
Indices of cusp erosion for vertical sections				
Erosion rate constant				
Index of backcutting ($\sin\theta_{max}$)	176	0·765	0·159	0·094–0·979
Index of lateral cusp movement‡	88	1·33	0·602	1·00–6·10
Erosion rate varying with slope				
Index of backcutting ($\sin\theta_{max}.\cos\theta_{max}$)	176	0·433	0·070	0·093–0·500
Index of lateral cusp movement‡	88	1·23	0·410	1·00–5·03

* Complete data are available for 88 cusps (i.e. 108–20). In the case of the indices of backcutting the data relate to the separate sides of the cusps
† Angle between the two slopes that form the cusp (i.e. $180-\theta_{max1}-\theta_{max2}$)
‡ Asymmetry ratio (higher : lower value) of the index of backcutting

Surface roughness (millimetre scale) of rillenkarren sides

The mean gradient change (MGC) values of the 44 rectilinear sides range from 1·5 to 20·8°, with an overall mean of 9·8° (Table II). By comparison, the parabolic sides are significantly smoother (*t*-test, $p<0{\cdot}001$), the mean adjusted MGC being 6·1°. In the case of the parabolic sides there are significant correlations between $\log_{10}$ adjusted MGC and both $\log_{10}$ depth ($r=0{\cdot}208$, $p<0{\cdot}01$) and $\log_{10}$ width ($r=0{\cdot}361$, $p<0{\cdot}001$). Thus, deeper and, particularly, wider parabolic sides tend to have rougher surfaces. There are no significant correlations between MGC and other morphometric properties for the rectilinear sides.

DISCUSSION

Representativeness of the study area

Previous studies have suggested that rillenkarren develop best on relatively pure, homogeneous, fine-grained strata (Ford and Lundberg, 1987; Goudie *et al*., 1989). However, the occurrence of such well developed rillenkarren on limestone breccias and conglomerates, with variable concentrations of insoluble impurities, shows that rillenkarren development can be supported on rocks that are quite impure and heterogeneous (Mottershead, 1996). The fine-grained nature of the matrix may be the key factor that favours rillenkarren development at this site (D. C. Ford, pers. comm.). The dimensions of the cross-sections studied are typical of those elsewhere. Thus, the mean width (18·2 mm) is within the 10 to 30 mm range reported in world-wide comparisons (Ford and Lundberg, 1987; Goudie *et al*., 1989), and the mean depth (4·2 mm) is almost identical to that on recrystallized limestone at Chillagoe, Queensland (Lundberg, 1977b, cited by Dunkerley, 1983). Moreover, visual comparisons with published profiles from other locations suggest that the form of the cross-sections at Lluc is also quite typical.

Variability of form

The results show that rillenkarren can exhibit marked local variability in cross-sectional form, even from one flute to the next across an outcrop. Variability in basic properties such as flute width and depth is evident from data presented in previous studies, and the ranges of widths (8·3 to 40·3 mm) and depths (0·9 to 13·1 mm) recorded at Lluc are broadly in keeping with those reported elsewhere. Published cross-sections of both natural (Dunkerley, 1979, p. 336; Goudie *et al*., 1989, p. 98) and simulated rillenkarren (Glew and Ford, 1980, p. 33) also show flutes with asymmetrical cross-sections, individual sides that appear to be rectilinear rather than parabolic, and irregular rather than smooth surfaces. Hitherto, however, attention has focused on idealized,

smooth and symmetrical cross-sections, and no attempt has been made to determine the magnitude and significance of ‘deviations’ in form.

Many of the rillenkarren at Lluc are asymmetrical, with the two sides of the flutes differing in either width (i.e. the channel is not located centrally) and/or depth (i.e. the cusp on one side is higher than the other). As a consequence, the mean slope from cusp to base often differs markedly between the two sides. Differences in steepness are also evident on either side of the cusps that separate adjacent flutes. The occurrence of such asymmetry dictates that cross-sections are best regarded as comprising two separate sides. These share a common base along the bottom of the flute, but their slope and watershed (cusp line) to some extent develop independently, much as do valley-side slopes. This independence of form is well illustrated by the fact that more than a third of the flutes studied have both a parabolic and rectilinear side. Also, there are often wide differences between opposite sides of flutes in terms of the goodness of fit (r^2 value) of the best-fit curves/lines and the degree of surface roughness (as reflected in the MGC index).

Implications for rillenkarren development

The fact that almost 80 per cent of the sides are parabolic, and that 105 of the 108 flutes contain at least one parabolic side, supports the theory that this is the characteristic form. In previous studies, curve-fitting has generally been restricted to flutes with parabolic cross-sections, and little consideration has been given to flutes that do not conform with theory. At Lluc, for example, Mottershead (1996, p. 22) only fitted curves to ‘the best formed single flute’ on each rock surface investigated. However, the present study shows that more than 20 per cent of the sides (e.g. 4B2 and 4C2, Figure 3) are not parabolic. Here these are termed ‘rectilinear’, though some of them actually fit more closely an inverted parabola centred over the cusp.

The rectilinear sides generally are less deeply incised and have rougher surfaces, which suggests they are less well developed forms. The fact that they do not increase in gradient upslope seems likely to be the result of ‘competition’ for space on the rock surface. Two circumstances may be envisaged. First, a lateral shift in the cusp line as one flute expands at the expense of another will lead to the loss of the upper segments of the side that is being encroached upon. Many of the cusps are markedly asymmetrical, with more than one-fifth of the differences in gradient being ≥20·0°. This asymmetry seems likely to be an important factor in the migration of cusp lines. Indeed, about two-fifths of the cusps have indices of lateral cusp movement of ≥1·20. Secondly, where the parabolic sides of flutes widen through time, they tend to develop a more extensive low-gradient basal section. Once these basal sections exceed a certain width (and possibly their slope is reduced below a critical angle), new flutes may develop. Initially they will take the form of minor irregularities nested within existing flutes, as appears to be the case with side 4C2 (Figure 3). In time, however, they will fully capture the upper part of the pre-existing side and develop as features in their own right. Clearly, both the above mechanisms will disrupt the characteristic parabolic form. Rectilinear sides may therefore be interpreted as either truncated or immature forms. Over time, many will develop into mature forms with parabolic sides. Equally, some existing parabolic sides will lose their distinctive form as a result of cusp migration and incipient flute formation. In this way sets of rillenkarren can be regarded as being in dynamic equilibrium. Thus, their overall dimensions (e.g. mean depth and width), the proportions of parabolic and rectilinear sides, etc. are likely to remain essentially constant over time. However, the detailed form of individual flutes constantly changes as the cusps (and presumably the flute bases) move laterally as the surface is lowered. Inevitably, some flutes are captured by others, but such losses may be compensated by the development of new flutes, nested within larger forms.

Unfortunately, the roughness of rillenkarren cross-sections has not been studied elsewhere. It is therefore not possible to assess whether the heterogeneity in rock composition at Lluc produces rougher surfaces. Comparisons may, however, be made with the results of a complementary study undertaken on the roughness of various other karren features (Crowther, 1997). The data for the long profiles of rillenkarren channels (central flute of set) and the downslope profiles of the ausgleichsflächen presented in Table V relate to the same 20 sites reported above. Comparable MGC data for the sets of cross-sections (excluding rectilinear sides) are shown. Surface roughness increases from the cross-sections (mean MGC, 5·9°) to the rillenkarren long profiles (8·6°), and then decreases to the ausgleichsflächen (6·9°), the difference in both cases being statistically significant (t-test, $p < 0{\cdot}001$).

Table V. Summary of MGC data (°) for the individual rock surfaces studied ($n = 20$). Only rillenkarren sides of parabolic form are included in the rillenkarren cross-section data, and these figures have been adjusted for curvature

	Mean	Std dev.	Range
Flute cross-sections	5·9	2·14	0·7–9·3
Flute channel long profiles*	8·6	1·60	6·1–13·2
Ausgleichsflächen*	6·9	0·90	5·2–8·6

* Data from Crowther (1997)

In general, karren formed by concentrated flow on steeper slopes have rougher surfaces than those associated with thin diffuse water films on gentle slopes (Crowther, 1997). This is presumed to reflect contrasts in the degree of turbulence. Where water flows over rock surfaces a thin 'boundary layer' of static water is present at the water/rock interface. This layer, which is thought to range from *c*. 1–1000 µm in thickness (Ford and Williams, 1989, p. 82), limits the rate of supply of reactants to, and removal of products from, the water/rock interface as dissolution takes place. Where flow is laminar the layer will be relatively thick, particularly in hollows in the rock surface. Any tendency for irregularities to develop as a result of local solubility contrasts is therefore countered by the more aggressive dissolution (due to a thinner boundary layer) of any resistant components that begin to form residual relief features. In contrast, where flow is more turbulent, the boundary layer is very thin, and this promotes preferential weathering of more soluble limestone to form an irregular surface.

The change in roughness downslope from the rillenkarren channels to the ausgleichsflächen seems to accord with these principles in that turbulence will tend to diminish as the lines of concentrated flow issue from the flutes and water spreads as a thin diffuse film over the ausgleichsflächen. In the case of the flute sides, it would be anticipated that direct raindrop impact would create considerable turbulence within what is inevitably a very thin water film, yet the parabolic sides are relatively smooth. Three factors might be important. First, dissolution will take place continuously within the thin film of slowly moving water that covers the rock surface during rainfall, whereas the duration of raindrop/rock contact at a particular point on the surface is very short indeed. Thus, whilst raindrops cause dissolution (directly) and promote dissolution within the existing water film by causing turbulence, and whilst raindrop impact is undoubtedly fundamental to the development of rillenkarren, a significant proportion of the actual dissolution of the flute sides seems likely to be associated with less turbulent flow. Secondly, the steep slopes of the sides in vertical section (Table II), combined with the parabolic shape, are assumed to be important. On such surfaces raindrops will be readily deflected into the deeper water in the channel at the base of the slope, thereby limiting the amount of disturbance within the thin water film on the sides. Both the above points apply equally well to rillenkarren on salt and gypsum as to those on limestone, and may explain why rillenkarren on gypsum often have sides that are very smooth in appearance (D. C. Ford, pers. comm.). Thirdly, as recent work by Fiol *et al*. (1996) has shown, algae can play a significant role in the weathering of rillenkarren on limestones in Mallorca by weakening the structure of the surface. In these circumstances, the physical force of raindrop impact may play an important role in shaping the rillenkarren by dislodging loosened particles. Certainly, any protrusions on the steeper sections of the sides will become foci for such attack, and this will presumably tend to favour the development of smooth surfaces. The fact that certain rillenkarren at Lluc extend through arenaceous pebbles with no substantial disruption of form (Figure 1b; Mottershead, 1996) further reinforces the idea that physical processes and controls are important in rillenkarren development.

CONCLUSIONS

The study at Lluc clearly demonstrates the advantages of obtaining precise measurements of the detailed form of rillenkarren cross-sections from profile gauge transects. Such data not only allow more rigorous analysis than has been achieved in previous qualitative and semi-quantitative studies, as for example in the fitting of curves to rillenkarren sides, but also facilitate the investigation of a wider range of morphometric characteristics, such as flute and cusp asymmetry, surface roughness and the properties of vertical sections. Methodologies for quantifying these characteristics have been developed and utilized in the present study.

The results highlight the pronounced width, depth and depth:width asymmetry of many flute cross-sections. Consequently, the flutes must be regarded as comprising two separate sides, with best-fit curves being derived independently for each, rather than for the cross-section as a whole. The predominance of sides with parabolic profiles confirms this as the characteristic shape. However, more than 20 per cent of the sides are rectilinear. These generally have rougher surfaces than the parabolic sides and are thought to be associated with truncated or immature forms. Many of the cusps are asymmetrical and consequently the cusp lines will tend to move laterally as erosion proceeds. On the basis of these findings it is argued that sets of rillenkarren can be regarded as being in dynamic equilibrium – their overall form remains essentially constant over time, but the detailed form of individual flutes changes as the cusp lines, and presumably the flute channels, shift position. Some flutes will be captured by others, whereas new flutes will develop, nested initially within larger ones. Dissolution is clearly a vital process in the development of rillenkarren. Indeed, on gypsum and experimental plaster of Paris blocks (in the absence of biological weathering) it is the only significant process. From the smoothness of the parabolic sides it is inferred that a significant proportion of dissolution occurs in water in which there is little turbulence. This might be attributable to the efficiency with which raindrops are deflected into the centre of the flute, thereby causing only limited disturbance within the film of water on the sides, and/or to the fact that much of the dissolution at a given point on the surface occurs within the water film in the time between successive raindrop impacts. In the case of rillenkarren on limestones, it might also be postulated that the physical force of raindrop impact contributes to the smoothness of the parabolic form by detaching tiny projecting rock fragments that have been weathered loose by biological agencies. Detailed process studies are needed to establish the precise mechanisms involved.

ACKNOWLEDGEMENTS

The author gratefully acknowledges the assistance of Helen Baker (digitizing), Ian Clewes (photographic work), Trevor Harris (diagrams) and Alan Rogers (computer programming). Constructive comments on an earlier version of this paper were received from Professor D. C. Ford and two anonymous referees.

REFERENCES

Crowther, J. 1984. 'Meso-scale topography and soil cover in tropical karst terrain, West Malaysia', *Zeitschrift für Geomorphologie, N.F.*, **28**, 219–234.

Crowther, J. 1996. 'Roughness (mm-scale) of limestone surfaces: examples from coastal and mountain karren features in Mallorca', in Fornós, J. J. and Ginés, À. (Eds), *Karren Landforms*, Proceedings of International Symposium on Karren Landforms, Soller, Mallorca, UIB Press, Mallorca, 149–160.

Crowther, J. (1997) 'Surface roughness and the evolution of karren forms at Lluc, Serra de Tramuntana, Mallorca', *Zeitschrift für Geomorphologie*, N.F., **41**, 393–407.

Dunkerley, D. L. 1979. 'The morphology and development of rillenkarren', *Zeitschrift für Geomorphologie, N.F.* **23**, 332–348.

Dunkerley, D. L. 1983. 'Lithology and micro-topography in the Chillagoe karst, Queensland, Australia', *Zeitschrift für Geomorphologie, N.F.* **27**, 191–204.

Fiol, Ll., Fornós, J. J. and Ginés, À. 1996. 'Effects of biokarstic process on the development of solutional rillenkarren in limestone rocks', *Earth Surface Processes and Landforms*, **21**, 447–452.

Ford, D. C. and Lundberg, J. 1987. 'A review of dissolutional rills in limestone and other soluble rocks', *Catena, Supplement*, **8**, 119–140.

Ford, D. C. and Williams, P. 1989. *Karst Geomorphology and Hydrology*, Unwin Hyman, London.

Glew, J. R. and Ford, D. C. 1980. 'A simulation study of the development of rillenkarren', *Earth Surface Processes*, **5**, 25–36.

Goudie, A. S., Bull, P. A. and Magee, A. W. 1989. 'Lithological control of rillenkarren development in the Napier Range, Western Australia, *Zeitschrift für Geomorphologie, Supplementband*, **75**, 95–114.

Haigh, M. J. 1981. 'Micro-profile measurement using the contour gauge', *British Geomorphological Research Group, Technical Bulletin*, **29**, 31–32.

Lundberg, J. 1977a. 'An analysis of the form of rillenkarren from the tower karst of Chillagoe, North Queensland, Australia', *Proceedings, 7th International Speleological Congress*, Sheffield, England, 294–296.

Lundberg, J. 1977b. *The geomorphology of Chillagoe limestones: variations with lithology*, unpublished MSc thesis, Australian National University, Canberra, 175 pp.

McCarroll, D. 1992. 'A new instrument and techniques for the field measurement of rock surface roughness', *Zeitschrift für Geomorphologie, N.F.* **36**, 69–79.

Mottershead, D. N. 1996. 'A study of solution flutes (Rillenkarren) at Lluc, Mallorca', *Zeitschrift für Geomorphologie, Supplementband*, **103**, 215–241.

Shaw, G. and Wheeler, D. 1985. *Statistical Techniques in Geographical Analysis*, Wiley, Chichester.

Vincent, P. J. 1983. 'The morphology and morphometry of some arctic trittkarren', *Zeitschrift für Geomorphologie*, **27**, 205–222.

